

# Synthesis and characterization of Co(II) and Ni(II) complexes of 2,5-diphenyl-3,4-bis(2-pyridyl)-cyclopentadienone (L). X-ray crystal structures of $\text{CoLCl}_2 \cdot 0.5\text{CH}_3\text{CN}$ and $\text{NiLBr}_2 \cdot \text{CHCl}_3$

Mehdi Amirnasr<sup>a,\*</sup>, Vratislav Langer<sup>b</sup>, Ahmad Amiri<sup>a</sup>, Shadpour Mallakpour<sup>a</sup>, Farzaneh Afshar<sup>a</sup>

<sup>a</sup> Department of Chemistry, Isfahan University of Technology, Isfahan 84156-83111, Iran

<sup>b</sup> Environmental Inorganic Chemistry, Department of Chemical and Biological Engineering, Chalmers University of Technology, SE-412 96 Gothenburg, Sweden

## ARTICLE INFO

### Article history:

Received 5 June 2009

Accepted 26 November 2009

Available online 1 December 2009

### Keywords:

Chelates

Cobalt(II)

Nickel(II)

Pseudotetrahedral

Crystal structures

## ABSTRACT

The preparation and properties of  $[\text{M}(\text{chelate})\text{X}_2]$  complexes are reported, where M = Co(II) or Ni(II), chelate = 2,5-diphenyl-3,4-bis(2-pyridyl)cyclopentadienone and X = Cl or Br. These complexes have been characterized by elemental analyses and spectroscopic methods. The crystal and molecular structures of  $\text{CoLCl}_2 \cdot 0.5\text{CH}_3\text{CN}$  (**1**) and  $\text{NiLBr}_2 \cdot \text{CHCl}_3$  (**4**) have been determined by X-ray crystallography. Compound (**1**) crystallizes in the triclinic space group  $P\bar{1}$ , different from that of  $\text{CoLCl}_2$  (monoclinic space group  $P2_1/c$ ) that we have reported previously. Compound (**4**) crystallizes in the monoclinic space group  $P2_1/n$ . Both  $\text{CoLCl}_2$  and  $\text{NiLBr}_2$  complexes are pseudo-tetrahedral, and utilization is made of the electronic and vibrational spectra in the structural diagnosis of  $\text{CoLBr}_2$  and  $\text{NiLCl}_2$ .

© 2009 Elsevier Ltd. All rights reserved.

## 1. Introduction

The formation and characterization of complexes of the type  $\text{MLX}_2$ , where M = Co(II), Ni(II), L = ligands formed by the linkage of two pyridine residues, in the ortho position, by various groups such as  $-\text{CH}_2\text{CH}_2-$ ,  $-\text{SS}-$ ,  $-\text{N}=\text{N}-$ ,  $-\text{NH}-$ , etc., and X = Cl, Br, I, NCS, have been the subject of considerable interest [1–8]. The ligands show unusual adaptability to different environments and result in the formation of structurally different complexes depending on their modes of coordination and the conformations of the coordinated L ligands. Steric effects and internal strain are expected to be different in these complexes and, depending on the structures of 1,2-di(2'-pyridyl) ligands and the stability of their compounds, synthetic conditions may vary from one group of complexes to another. In this paper we report the synthesis and characterization of a series of new  $\text{MLX}_2$  complexes with internal strain imparted by the structurally rigid L ligand, Scheme 1. We also report the X-ray structural analysis of  $\text{CoLCl}_2 \cdot 0.5\text{CH}_3\text{CN}$  and  $\text{NiLBr}_2 \cdot \text{CHCl}_3$  complexes.

## 2. Experimental

### 2.1. Materials

Solvents and starting materials were obtained from Fluka and Aldrich and used as received. The red ligand L was prepared by

thermal dehydration of its white diol precursor,  $\text{LH}_2(\text{OH})_2$ , over silica gel as reported elsewhere [9]. Electronic spectra in solution were recorded on a JASCO V-570 spectrophotometer. IR spectra were recorded as KBr pellets on a FT-IR JASCO 680 PLUS instrument. Elemental analyses were performed by using a Perkin-Elmer 2400II CHNS/O analyzer.

### 2.2. Synthesis of complexes

#### 2.2.1. $\text{CoLCl}_2 \cdot 0.5\text{CH}_3\text{CN}$ (**1**)

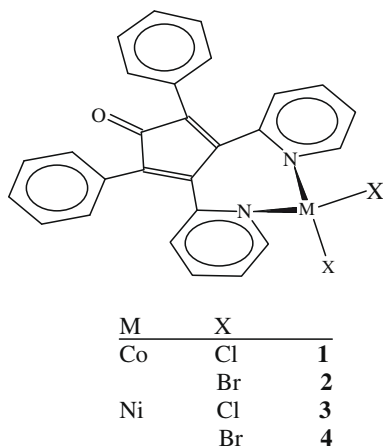
A solution of the ligand L (0.193 g, 0.5 mmol) in chloroform (40 mL) was added to a suspension of  $\text{CoCl}_2$  (0.091 g, 0.7 mmol) in chloroform (10 mL). The reaction mixture was stirred at room temperature for 3 h to give a cherry red solution. The unreacted  $\text{CoCl}_2$  was removed by filtration and the filtrate was left in the hood for two days to give dark red crystals of  $\text{CoLCl}_2$  in 95% yield (based on the ligand L). The product was recrystallized from a mixture of chloroform–acetonitrile (20:1 v/v) to give dark crystals of X-ray quality which were washed and dried in air. *Anal.* Calc. for  $\text{C}_{27}\text{H}_{18}\text{Cl}_2\text{CoN}_2\text{O} \cdot 0.5\text{CH}_3\text{CN}$ : C, 62.65; H, 3.66; N, 6.52. Found: C, 62.4; H, 3.60; N, 6.60%. IR (KBr pellets,  $\nu/\text{cm}^{-1}$ ):  $\nu(\text{C}=\text{O})$  1715(s);  $\nu(\text{C}=\text{N py})$  and  $\nu(\text{C}=\text{C aromatic})$  1599, 1566, 1493, 1473, 1440(m);  $\nu(\text{C}\equiv\text{N acetonitrile})$  2250(w).

#### 2.2.2. $\text{CoLBr}_2$ (**2**)

This complex was prepared as described for compound **1** except that stoichiometric amounts of  $\text{CoBr}_2$  and L (0.5 mmol) were used

\* Corresponding author. Tel.: +98 311 3912351; fax: +98 311 3912350.

E-mail address: [amirnasr@cc.iut.ac.ir](mailto:amirnasr@cc.iut.ac.ir) (M. Amirnasr).



**Scheme 1.** Structural formulas of the complexes.

and the reaction mixture was stirred for 12 h. Red purple needle like crystals of  $\text{CoBr}_2$  were obtained in 73% yield (based on the ligand L) from the final filtrate after two days. The product was recrystallized from chloroform and dried in air. *Anal. Calc.* for  $\text{C}_{27}\text{H}_{18}\text{Br}_2\text{CoN}_2\text{O}$ : C, 53.59; H, 3.00; N, 4.63. Found: C, 53.90; H, 3.00; N, 4.40%. IR (KBr pellets,  $\nu/\text{cm}^{-1}$ ): 3050  $\nu(\text{CH})$ ;  $\nu(\text{C=O})$  1718(s);  $\nu(\text{C=N py})$  and  $\nu(\text{C=C aromatic})$  1595, 1560, 1490, 1470, 1440(m).

### 2.2.3. $\text{NiCl}_2$ (3)

This complex was prepared as described for compound (1) except that  $\text{NiCl}_2$  was used in excess ( $\text{Ni/L} \cong 2$ , 1/0.5 mmol), and the reaction mixture in chloroform was stirred for 60 h. The product

**Table 1**  
Crystal and structure refinement data for  $\text{CoCl}_2 \cdot 0.5\text{CH}_3\text{CN}$  (1) and  $\text{NiBr}_2 \cdot \text{CHCl}_3$  (4).

Compound	1	4
Empirical formula	$\text{C}_{56}\text{H}_{39}\text{Cl}_4\text{Co}_2\text{N}_5\text{O}_2$	$\text{C}_{28}\text{H}_{19}\text{Br}_2\text{Cl}_3\text{NiN}_2\text{O}$
Formula weight	1073.58	724.33
T (K)	153(2)	153(2)
Crystal system	triclinic	monoclinic
Crystal size (mm)	$0.94 \times 0.22 \times 0.08$	$0.68 \times 0.18 \times 0.17$
Space group	$P\bar{1}$	$P2_1/n$
a (Å)	8.7243(4)	7.0124(14)
b (Å)	16.6040(8)	21.595(4)
c (Å)	17.7740(9)	18.916(4)
$\alpha$ (°)	77.328(1)	90
$\beta$ (°)	84.773(1)	96.041(4)
$\gamma$ (°)	77.157(1)	90
V (Å <sup>3</sup> )	2446.7(2)	2848.7(10)
Z, $D_{\text{calc}}$ ( $\text{g cm}^{-3}$ )	2, 1.457	4, 1.689
$\mu$ ( $\text{mm}^{-1}$ )	0.945	3.793
F(0 0 0)	1096	1432
$\theta$ Range for data collection (°)	2.35–33.08	2.17–28.67
Index ranges	$-13 \leq h \leq 13$ $-25 \leq k \leq 25$ $-27 \leq l \leq 26$	$-9 \leq h \leq 9$ $-29 \leq k \leq 29$ $-25 \leq l \leq 25$
Reflections collected	44678	39897
Independent reflections	17336	7291
$R_{\text{int}}$	0.0226	0.0524
Completeness to $\theta$ (°)	31.00, 99.5%	28.67, 99.3%
Maximum and minimum transmission	0.9282, 0.7153	0.5648, 0.1983
Data/parameters	17336/623	7291/334
Good-of-fit on $F^2$	1.002	1.008
$R_1/wR_2$ for observed reflection [ $I > 2\sigma(I)$ ]	0.0315/0.0822	0.0401/0.0945
$R_1/wR_2$ for all data	0.0419/0.0873	0.0623/0.1074
Largest resolution peak/hole ( $\text{e} \text{ \AA}^{-3}$ )	0.566/−0.272	1.037/−0.692

was obtained as a red purple powder in 70% yield (based on the ligand L). The complex was recrystallized from dichloromethane and dried in air. *Anal. Calc.* for  $\text{C}_{27}\text{H}_{18}\text{Cl}_2\text{NiN}_2\text{O}$  (516.05): C, 62.84; H, 3.52; N, 5.43. Found: C, 62.70; H, 3.40; N, 5.32%. IR (KBr pellets,  $\nu/\text{cm}^{-1}$ ):  $\nu(\text{C=O})$  1717(s);  $\nu(\text{C=N py})$  and  $\nu(\text{C=C aromatic})$  1599, 1567, 1494, 1473, 1442(m).

### 2.2.4. $\text{NiBr}_2 \cdot \text{CHCl}_3$ (4)

This complex was prepared as described for compound 1 except that stoichiometric amounts of  $\text{NiBr}_2$  and L (0.5 mmol) were used

**Table 2**  
Electronic absorption spectral data for 1–4 and the red L,  $\lambda/\text{nm}$  ( $\epsilon/\text{L mol}^{-1} \text{ cm}^{-1}$ ).

$\text{CoCl}_2$ (1)	$\text{CoBr}_2$ (2)	$\text{NiCl}_2$ (3)	$\text{NiBr}_2$ (4)	Red L
254 (24324)	255 (21830)	260 (17860)	255 (18700)	258(20090)
287 (12622)	288 (12341)	292 (11800)	296 (14000)	324(5012)
360 (3250)	360 (3162)	360 (2850)	360 (2540)	492(1167)
510 (1488)	512 (1625)	521 (1504)	526 (1700)	
569 (1183)	594 (1112)	852 (10)	888 (26)	
610 (795)	626 (895)	984 (44)	1007 (51)	
650 (465)	664 (626)			
985 (19)	1020 (24)			
1340 (73)	1400 (112)			

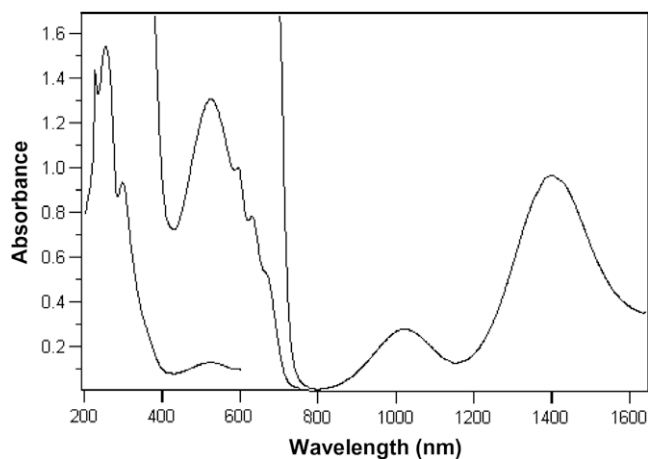


**Fig. 1.** UV-Vis spectrum of  $\text{CoBr}_2$  (400–200 nm,  $7.1 \times 10^{-5}$  M; 800–400 nm,  $8.0 \times 10^{-4}$  M; 1600–800 nm,  $8.8 \times 10^{-3}$  M) in  $\text{CH}_2\text{Cl}_2$ .

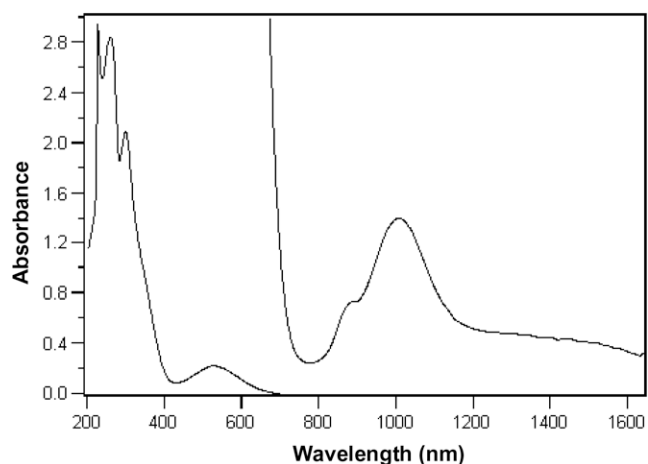


**Fig. 2.** UV-Vis spectrum of  $\text{NiBr}_2$  (700–200 nm,  $1.5 \times 10^{-4}$  M; 1600–700 nm,  $2.45 \times 10^{-2}$  M) in  $\text{CH}_2\text{Cl}_2$ .

and the reaction mixture was stirred for 12 h. Red purple needle like crystals of  $\text{NiLBr}_2$  were obtained in 73% yield (based on the ligand L) from the final filtrate after two days. The product was recrystallized from chloroform and dried in air. *Anal. Calc.* for  $\text{C}_{27}\text{H}_{18}\text{Br}_2\text{NiN}_2\text{O}\cdot\text{CHCl}_3$ : C, 46.43; H, 2.64; N, 3.87. *Found*: C, 46.90; H, 2.60; N, 3.80%. IR (KBr pellets,  $\nu/\text{cm}^{-1}$ ):  $\nu(\text{C}=\text{O})$  1717(s);  $\nu(\text{C}=\text{N py})$  and  $\nu(\text{C}=\text{C aromatic})$  1599, 1567, 1493, 1473, 1442(m).

### 2.3. X-ray crystallography

Data were collected on a Siemens SMART CCD diffractometer equipped with LT-2A low temperature device, using graphite-monochromated  $\text{Mo K}\alpha$  ( $\lambda = 0.71073 \text{ \AA}$ ) radiation. A full sphere of reciprocal lattice was scanned by  $0.3^\circ$  steps in  $\omega$  with a crystal-to-detector distance of 3.97 cm. Preliminary orientation matrices were obtained from the first frames using SMART [10]. The frames were integrated using the preliminary orientation matrices which were updated every 100 frames. Final cell parameters were obtained by the refinement on the positions of 7108 and 6109 (for **1** and **4**, respectively) reflections with  $I > 2\sigma(I)$ , after integration of all the frames using SAINT [10]. The data were empirically corrected for absorption and other effects using SADABS [11]. The structures were solved by direct methods and refined by the full-matrix least-squares method on  $F^2$  data using the SHELXTL [12]. All non-H atoms were refined anisotropically. The H atoms were constrained to idealized geometries and refined isotropically. The crystallographic and refinement data are summarized in Table 1.

## 3. Results and discussion

### 3.1. Synthesis of complexes

The  $\text{MLX}_2$  complexes were prepared by the reaction of the appropriate metal halide with the bidentate ligand L (Scheme 1). The synthesis of  $\text{CoLX}_2$  and  $\text{NiLX}_2$  complexes were carried out in chloroform. The procedure reported in the literature for the synthesis of related cobalt and nickel complexes in ethanol [1] proved to be unsuccessful for the preparation of  $\text{CoLX}_2$  and  $\text{NiLX}_2$ . This is due to the steric factors imposed by the more rigid structure of the ligand L as compared to the related ligands in Ref. [1]. From a structural point of view the N–N bite of the chelating ligands is controlled by the linkage between the two pyridine rings. Furthermore, the kinetic chelate strain effect [13] which arises from the

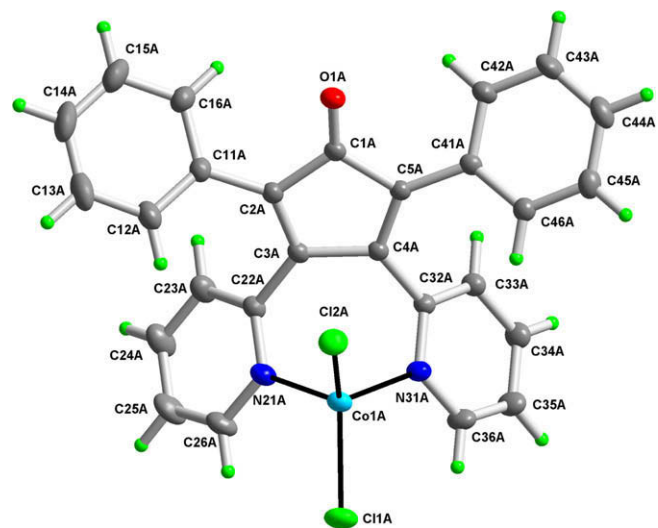


Fig. 3A. Numbering of molecule **1A** together with atomic displacement ellipsoids drawn at 50% probability level.

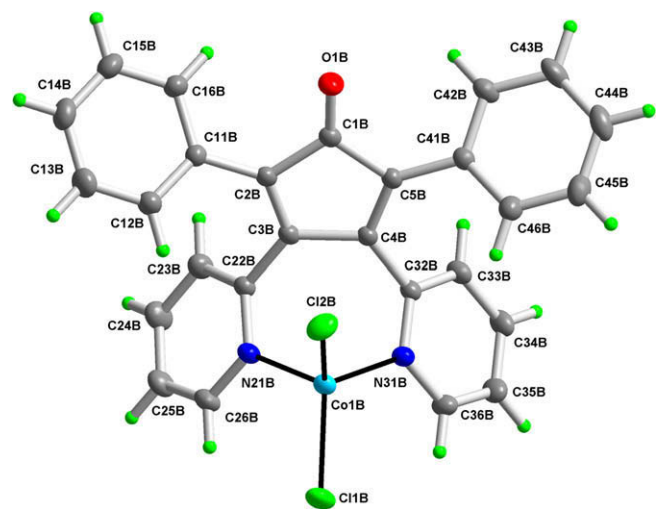


Fig. 3B. Numbering of molecule **1B** together with atomic displacement ellipsoids drawn at 50% probability level.

Table 3  
Selected bond distances ( $\text{\AA}$ ), bond and torsion angles ( $^\circ$ ) in **1** and **4**.

<b>1A</b>	<b>1B</b>	<b>4</b>			
Bond distances					
Co1A–N21A	2.0270(11)	Co1B–N21B	2.0483(10)	Ni–N21	2.008(2)
Co1A–N31A	2.0297(10)	Co1B–N31B	2.0330(10)	Ni–N31	2.018(3)
Co1A–Cl1A	2.2328(4)	Co1B–Cl1B	2.2223(4)	Ni–Br1	2.3745(6)
Co1A–Cl2A	2.2166(3)	Co1B–Cl2B	2.2248(4)	Ni–Br2	2.3546(6)
Bond angles					
N21A–Co1A–N31A	93.71(4)	N21B–Co1B–N31B	93.93(4)	N21–Ni–N31	94.84(9)
N21A–Co1A–Cl2A	112.64(3)	N21B–Co1B–Cl2B	112.64(3)	N21–Ni–Br2	110.58(7)
N31A–Co1A–Cl2A	114.14(3)	N31B–Co1B–Cl2B	114.26(3)	N31–Ni–Br2	111.28(7)
N21A–Co1A–Cl1A	108.92(3)	N21B–Co1B–Cl1B	109.57(3)	N21–Ni–Br1	104.50(7)
N31A–Co1A–Cl1A	109.51(3)	N31B–Co1B–Cl1B	111.10(3)	N31–Ni–Br1	106.19(7)
Cl2A–Co1A–Cl1A	115.726(15)	Cl2B–Co1B–Cl1B	113.682(15)	Br2–Ni–Br1	125.08(2)
Torsion angles					
Co1A–N21A–C22A–C3A	–3.80(15)	Co1B–N21B–C22B–C3B	–9.23(14)	Ni–N21–C22–C3	–6.1(3)
Co1A–N31A–C32A–C4A	8.98(14)	Co1B–N31B–C32B–C4B	9.71(14)	Ni–N31–C32–C4	1.3(3)
N21A–C22A–C3A–C4A	55.83(16)	N21B–C22B–C3B–C4B	61.54(15)	N21–C22–C3–C4	55.5(4)
N31A–C32A–C4A–C3A	–59.51(15)	N31B–C32B–C4B–C3B	–59.51(15)	N31–C32–C4–C3	–53.6(4)
C22A–C3A–C4A–C3A	0.71(17)	C22B–C3B–C4B–C3B	–2.10(17)	C22–C3–C4–C32	1.3(4)

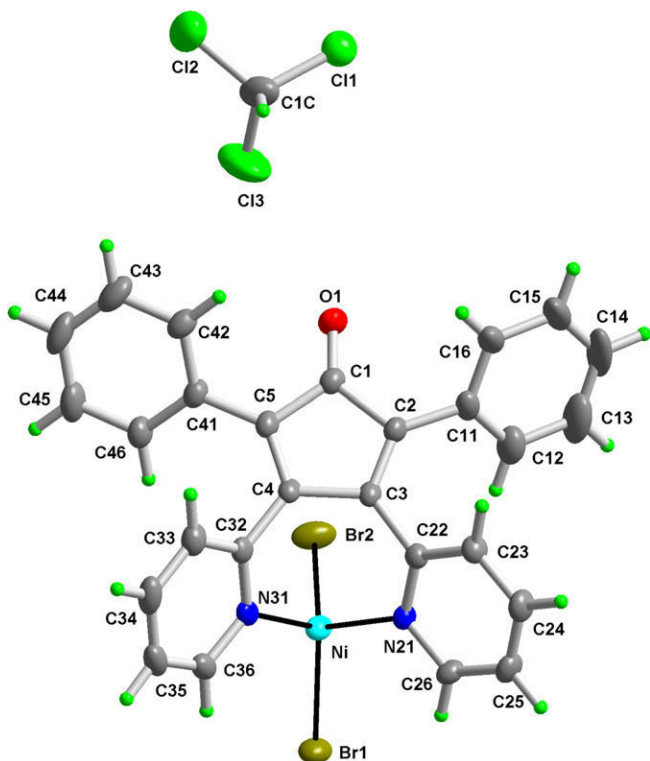


Fig. 4. Numbering scheme of molecule **4** with atomic displacement ellipsoids drawn at 50% probability level.

increase in M–N bond distance and the solvent interaction with metal ions are both operative in the process of complex formation. In ethanol (as well as in other polar and coordinating solvents), it is likely that the cobalt and nickel complexes exist in multiple equilibria with strongly solvated species that compete with  $MLX_2$  formation. The solubility and higher stability of these complexes in chloroform, make it ideal to run the reactions in this solvent.

### 3.2. Spectral characterization

The IR spectra of the complexes containing pyridine residues have been studied and used by other researchers to determine the coordination mode for the pyridine rings [14]. The  $MLX_2$  complexes have been divided into three series according to their infrared spectra. The infrared spectra of the series I in which the bidentate ligand has a *cis* conformation is more simple than others. This is indicative of the presence of a ligand having both pyridine residues coordinated to the metal in such a form that the pyridine groups are chemically equivalent.

The solid-state IR spectra of the cobalt and nickel complexes display several features that are supportive of a common coordination mode for the ligand L. The ketone  $C=O$  stretching mode observed at  $1715\text{ cm}^{-1}$  in the free ligand L, is observed as a single sharp band at about  $1717\text{ cm}^{-1}$  in all four complexes. The pyridine  $C=N$  and aromatic  $C=C$  stretching modes are shifted to higher frequencies by 5–15  $\text{cm}^{-1}$  in the complexes relative to the free ligand. Additional shifts are expected for the ring breathing mode which occurs at  $990\text{ cm}^{-1}$  in the free ligand and appears at  $1020\text{--}1025\text{ cm}^{-1}$  in the IR spectra of the complexes.

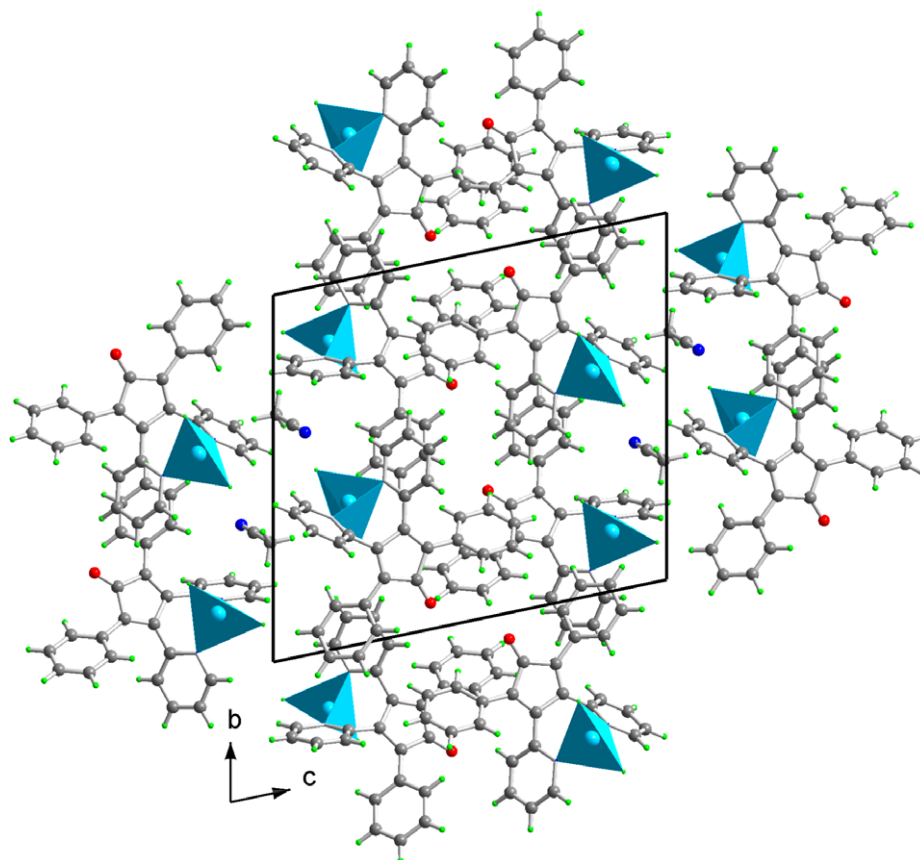


Fig. 5. Projection of the structure of **1** along the *a*-axis. Coordination tetrahedra of Co atoms are shown in blue. (For interpretation of the references to colour in this figure legend, the reader is referred to the web version of this article.)

The electronic absorption spectral data of the ligand L and its metal complexes are listed in Table 2. The ligand is a deep red solid and its solution in acetonitrile has a strong absorption at 492 nm ( $\epsilon = 1167$ ) assigned to a  $n \rightarrow \pi^*$  transition arising from the interaction of the ketone oxygen lone pairs with the  $\pi$  system of the molecule. This transition is slightly red shifted when the pyridines are protonated (512 nm) or coordinated to the metal ions (510–526 nm). The absorption at wavelengths less than 400 nm in the ligand are assigned to  $\pi \rightarrow \pi^*$  transitions of the rings. Additional CT transitions are expected for the metal complexes which appear below 400 nm. The ligand field transitions for  $\text{CoLCl}_2$  (**1**) and  $\text{CoLBr}_2$  (**2**) complexes (Fig. 1) include the intense multicomponent bands in the near-infrared region ( $6000\text{--}11000\text{ cm}^{-1}$ ) and in the visible region ( $14500\text{--}22000\text{ cm}^{-1}$ ) as expected for a pseudotetrahedral stereochemistry [15].

The electronic spectra of nickel complexes,  $\text{NiLCl}_2$  (**3**) and  $\text{NiLBr}_2$  (**4**), (Table 2) is consistent with a pseudotetrahedral structure (Fig. 2). The broad absorption bands near  $7000\text{ cm}^{-1}$  (components of  ${}^3T_2$ ) and  $10000\text{ cm}^{-1}$  ( ${}^3A_2$ ) and the shoulder at  $17000\text{ cm}^{-1}$  (components of  ${}^3T_1(P)$ ) which overlaps with the  $n \rightarrow \pi^*$  of the ligand are in accord with a  $C_{2v}$  symmetry of these complexes [15]. On the basis of the striking similarity of the spectroscopic properties of  $\text{CoLBr}_2$  (**2**) and  $\text{NiLCl}_2$  (**3**) complexes with those of  $\text{CoLCl}_2$  (**1**) and  $\text{NiLBr}_2$  (**4**) for which the X-ray structures have been determined (*vide infra*) a similar structure can also be inferred for (**2**) and (**3**) complexes.

### 3.3. Crystal and molecular structures of (**1**) and (**4**)

The crystallographic and refinement data are summarized in Table 1 and the selected bond distances, bond and torsion angles are given in Table 3. The molecular structures of (**1**) and (**4**) are illustrated in Figs. 3A, 3B and 4, respectively with metal atoms coordinated by the bidentate bis(2-pyridyl) ligand and two halogen atoms.

The structure of  $\text{CoLCl}_2 \cdot 0.5\text{CH}_3\text{CN}$  (**1**) consists of two, chemically identical but conformationally different molecules in the asymmetric unit. A highly puckered seven-membered chelation ring is formed with endocyclic torsion angles presented in Table 3. The average Co–N [2.034(10) Å] and Co–Cl [2.224(7) Å] bond distances and the N–Co–N [93.82(16)°] and Cl–Co–Cl [114.7(14)°] bond angles conform to those reported for the related complex [dichloro(2,5-diphenyl-3,4-di-2-pyridyl-1H-pyrrole-*N,N'*)cobalt(II)] [2]. The structural parameters such as the crystal system, space group, unit cell dimensions, and the crystal packing of compound (**1**) (trigonal, space group  $P\bar{1}$  and  $Z = 2$ ) are different from those of  $\text{CoLCl}_2$  (monoclinic, space group  $P2_1/c$ ,  $Z = 4$ ), that we have reported previously [16]. Compound (**1**) involves solvent molecules in its unit cell, which is apparently the source of these structural differences.

It is interesting to compare the structure of  $\text{CoLCl}_2$  (**1**) with that of the unchelated analogue,  $\text{Co(3-pic)}_2\text{Cl}_2$  [17]. The two structures are similar, with pseudotetrahedral cobalt coordination. However, the N–Co–N angle is  $104.19(8)^\circ$  in the unchelated complex whereas it is  $93.71(4)^\circ$  and  $93.93(4)^\circ$  in the chelate  $\text{CoLCl}_2$ . This large deviation is presumably the source of some strain in the structure of the complex, leading to the release of the L ligand in strongly coordinating solvents.

The  $\text{NiLBr}_2$  complex (**4**) also adopts a pseudotetrahedral structure where the tetrahedron is somewhat distorted by a small N–Ni–N angle being  $94.84(9)^\circ$ . The Br–Ni–Br angle has opened up to  $125.08(2)^\circ$ . The Ni–N distances ranging from 2.008(2) to 2.018(3) Å are considered normal and comparable to those for (**1**) and related complexes [2,16]. The average Ni–Br distance of 2.365(14) Å agrees well with normal Ni–Br bond distances in the related complex,  $\text{Ni(Phca}_2\text{en)Br}_2$  [18]. As in  $\text{CoLCl}_2$  (**1**), the seven

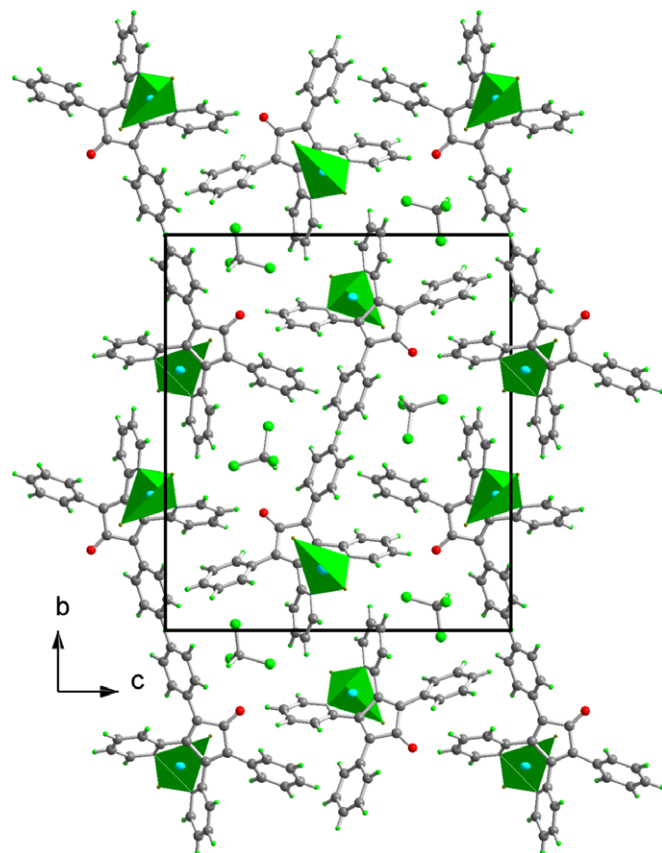


Fig. 6. Projection of the structure of **4** along the  $a$ -axis. Coordination tetrahedra of Ni atoms are shown in green. (For interpretation of the references to colour in this figure legend, the reader is referred to the web version of this article.)

membered ring is highly puckered with endocyclic torsion angles given in Table 3.

The packing of both compounds in the crystals is very different and it is shown in Fig. 5 and 6. In crystal structure of (**1**), there is apart from weak hydrogen bond of C–H $\cdots$ Cl, C–H $\cdots$ N and C–H $\cdots$ O types a quite strong  $\pi$ – $\pi$  interaction present between the aromatic phenyl rings C41A $\cdots$ C46A and C41B $\cdots$ C46B (symmetry operation:  $2 - x, 1 - y, 1 - z$ ) with a centroid–centroid distance of 3.7185(8) Å. In crystal structure of (**2**), there are weak H-bond interactions of type C–H $\cdots$ Br present, but no  $\pi$ – $\pi$  interaction was observed there. Instead, a C–H $\cdots$  $\pi$  interaction between the chloroform molecule and the phenyl ring C41 $\cdots$ C26, with hydrogen atom distance to the centroid of this ring being 2.83 Å, has been recognized.

## 4. Conclusion

The present study revealed tetrahedral geometry around Co(II) and Ni(II), where the metal atoms are coordinated by the bidentate bis(2-pyridyl) ligand and two halogen atoms. These complexes proved to be unstable in strongly coordinating solvents, presumably due to the strain imparted by the structurally rigid L ligand. A convenient method of synthesis for the preparation of these complexes in chloroform was concluded.

## Supplementary data

CCDC 661283 and 661284 contain the supplementary crystallographic data for **1** and **4**. These data can be obtained free of charge via <http://www.ccdc.cam.ac.uk/conts/retrieving.html>, or from the

Cambridge Crystallographic Data Centre, 12 Union Road, Cambridge CB2 1EZ, UK; fax: (+44) 1223-336-033; or e-mail: deposit@ccdc.cam.ac.uk.

### Acknowledgement

Partial support of this work by the Isfahan University of Technology Research Council is gratefully appreciated.

### References

- [1] M. Keeton, A.B. Lever, *Inorg. Chem.* 10 (1971) 47.
- [2] B. Viossat, N.-H. Dung, J. Lehuède, J.M. Vierfond, *Acta Crystallogr., Sect. C* 50 (1994) 211.
- [3] Y.-Z. Zhu, Z.-P. Li, J.-A. Ma, F.-Y. Tang, L. Kang, Q.-L. Zhou, A.S.C. Chan, *Tetrahedron: Asymmetry* 13 (2002) 161.
- [4] A. Panunzi, V. De Felice, N. Fraldi, G. Roviello, F. Ruffo, *Inorg. Chem. Commun.* 8 (2005) 1049.
- [5] W.M. Teles, M.V. Marinho, M.I. Yoshida, N.L. Speziali, K. Krambrock, C.B. Pinheiro, N.M. Pinhal, A.A. Leitão, F.C. Machado, *Inorg. Chim. Acta* 359 (2006) 4613.
- [6] S. Delgado, A. Barrilero, A. Molina-Ontoria, M.E. Medina, C.J. Pastor, Reyes Jiménez-Aparicio, J.L. Priego, *Eur. J. Inorg. Chem.* (2006) 2746.
- [7] M. Wriedt, I. Jess, C. Näther, *Acta Crystallogr., Sect. E* 64 (2008) m83.
- [8] C. Zhang, L. Yuan, J.-Y. Liu, W. Xu, *Acta Crystallogr., Sect. E* 65 (2009) o1213.
- [9] M. Amirnasr, A. Gorji, *Thermochim. Acta* 354 (2000) 31.
- [10] SMART and SAINT: Area Detector Control and Integration Software, Bruker AXS Inc., Madison, WI, USA, 2003.
- [11] G.M. Sheldrick, SADABS: Program for Empirical Absorption Correction for Area Detectors, Version 2.10, University of Göttingen, Germany, 2003.
- [12] G.M. Sheldrick, SHELXTL: Structure Determination Programs (Version 6.14), *Acta Crystallogr., Sect. A* 64 (2008) 112.
- [13] T.S. Turan, D.B. Rorabacher, *Inorg. Chem.* 11 (1972) 288.
- [14] D.A. Baldwin, A.B.P. Lever, R.V. Parish, *Inorg. Chem.* 8 (1969) 107.
- [15] A.B.P. Lever, *Inorganic Electronic Spectroscopy*, second ed., Elsevier, The Netherlands, 1984. p. 497 and 531.
- [16] A.D. Khalaji, M. Amirnasr, J.-C. Daran, *Acta Crystallogr., Sect. E* 62 (2006) m687.
- [17] D. Wyrzykowski, E. Styczeń, Z. Warnke, *Transition Met. Chem.* 31 (2006) 860.
- [18] M. Amirnasr, A.H. Mahmoudkhani, A. Gorji, S. Dehghanpour, H.R. Bijanzadeh, *Polyhedron* 21 (2002) 2733.